HHS Public Access

Author manuscript

Photochem Photobiol. Author manuscript; available in PMC 2018 July 01.

Published in final edited form as:

Photochem Photobiol. 2017 July ; 93(4): 1115–1122. doi:10.1111/php.12719.

A Comparison of Dose Metrics to Predict Local Tumor Control for Photofrin-mediated Photodynamic Therapy

Haixia Qiu[1,2], **Michele M. Kim**[1,3], **Rozhin Penjweini**[1], **Jarod C. Finlay**[1], **Theresa M. Busch**[1], **Tianhao Wang**[4], **Wensheng Guo**[4], **Keith A. Cengel**[1], **Charles B. Simone II**[1], **Eli Glatstein**[1], and **Timothy C. Zhu**[1,*]

[1]Department of Radiation Oncology, University of Pennsylvania, Philadelphia, PA

[2]Department of Laser Medicine, Chinese PLA General Hospital, Beijing

[3]Department of Physics and Astronomy, University of Pennsylvania, Philadelphia, PA

[4]Department of Biostatistics, University of Pennsylvania, Philadelphia, PA

Abstract

This preclinical study examines light fluence, PDT dose, and "apparent reacted singlet oxygen", $[^1O_2]_{rx}$, to predict local control rate (*LCR*) for Photofrin-mediated photodynamic therapy (PDT) of radiation-induced fibrosarcoma (RIF) tumors. Mice bearing RIF tumors were treated with in-air fluences (50–250 J/cm^2) and in-air fluence rates (50–150 mW/cm^2) at Photofrin dosages of 5 and 15 mg/kg and a drug-light interval of 24 hours using a 630nm 1-cm diameter collimated laser. A macroscopic model were used to calculate $[^1O_2]_{rx}$ and PDT dose based on *in vivo* explicit dosimetry of the drug concentration, light fluence, and tissue optical properties. PDT dose and $[^1O_2]_{rx}$ were defined as a temporal integral of drug concentration and fluence rate, and singlet oxygen concentration consumed divided by the singlet oxygen lifetime, respectively. *LCR* was stratified for different dose metrics for 74 mice (66 + 8 control). Complete tumor control at 14 days was observed for $[^1O_2]_{rx} \geq 1.1$ mM or PDT dose ≥ 1200 μMJ/cm^2 but cannot be predicted with fluence alone. *LCR* increases with increasing $[^1O_2]_{rx}$ and PDT dose but is not well correlated with fluence. Comparing dosimetric quantities, $[^1O_2]_{rx}$ outperformed both PDT dose and fluence in predicting tumor response and correlating with *LCR*.

INTRODUCTION

Photofrin-mediated photodynamic therapy (PDT) is approved by the US Food and Drug Administration (FDA) for the treatment of some malignant and pre-malignant conditions, such as esophageal cancer and non-small cell lung cancer (1–4). Photofrin is excited by exposure to light of a specific wavelength (usually at 400, 514, or 630 nm). Following the absorption of light, the photosensitizer undergoes a transition from its ground state (singlet state) into a relatively long-lived electronically excited state (triplet state) via a short-lived excited singlet state. The triplet can transfer its energy directly to ground-state oxygen ($^3O_2$) to form singlet-state oxygen ($^1O_2$), which is thought to be responsible for cell death and

*Corresponding author: tzhu@mail.med.upenn.edu (Timothy C. Zhu).

contributes to the clinical benefits of PDT (5). Because of the high reactivity and short half-life of $^1O_2$, only sub-cellular organelles within cells that are proximal to the area of the $^1O_2$ production (area of photosensitizer localization) are directly affected by PDT (6, 7). Therefore, PDT destroys the disease in a way that causes significantly less generalized or secondary toxicities than other conventional treatments such as surgery, chemotherapy, and ionizing radiation.

An ideal dosimetric predictor for PDT efficacy is still elusive due to the dynamic changes and interactions of the key PDT components (fluence, drug concentration, and oxygen level) during treatment, which, to some extent, has hindered the clinical application of PDT. In most clinical and pre-clinical protocols, PDT dosimetry is still based on the administered photosensitizer dosage and the delivered light fluence under a range of fluence rates (ϕ) (8, 9). This method of clinical dosimetry does not take into account actual levels of photosensitizer uptake in the target tissue or, more importantly, variations in photochemical PDT oxygen consumption variation for different ϕ during PDT (10, 11). An earlier study demonstrated that these factors may be responsible for the poor predictive power of current methods in clinical dosimetry (10, 11). PDT dose, which can be expressed as a product of photosensitizer concentration and ϕ, measures the photon energy absorbed by the photosensitizer (12). This quantity may serve as a good predictor of outcomes in $^3O_2$-rich conditions. However, under hypoxic conditions, it is less accurate in predicting PDT efficacy because it does not consider the rate of PDT consumption of $^3O_2$ for different ϕ (13). The formation of reactive oxygen species is critical to PDT efficacy. For type I sensitizers, hydroxyl radicals ($OH^{\bullet}$) appear to be the major cytotoxic element, but $^1O_2$ is likely responsible for cellular killing and clinical outcomes for type II photosensitizers such as Photofrin. As the primary mediator of cell damage during Photofrin-PDT, $^1O_2$ has gained special attention as a good dosimetric quantity based on either direct measurements or indirect modeling (14–17). This study is focused on the latter method due to the difficulties in directly measuring $^1O_2$ *in vivo* during PDT delivery. We use a singlet oxygen explicit dosimetry (SOED) method to calculate the concentration of reacted singlet oxygen, $[^1O_2]_{rx}$, by using an empirical five-parameter model. Calculated $[^1O_2]_{rx}$ is also compared with light fluence and PDT dose as dosimetric predictors for PDT. The tumor local control rate (LCR) is used as the treatment endpoint. Moreover, we provide Kaplan-Meier data analysis with in-depth statistical tests for the evaluation of the three dose metric quantities. To our knowledge, we are the first to establish the superiority of calculated $[^1O_2]_{rx}$ as a predictor of outcome to Photofrin-PDT *in vivo*, compared to light fluence or PDT dose.

MATERIALS AND METHODS

In vivo treatment protocols

Radiation-induced fibrosarcoma (RIF) cells in logarithmic growth phase (30 μl of 1×10^7 cells/ml concentration) were injected subcutaneously over the right shoulders of 6–8 week old female C3H mice (Charles River, Frederick, MD). Around 5–10 days after inoculation, when tumors reached ~3–5 mm in length, Porfimer Sodium (Photofrin©, Pinnacle Biologics, Chicago, Illinois) was injected at doses of 5 or 15 mg/kg via the tail vein. These doses of Photofrin were chosen to produce PDT doses that were well separated. At a 24 hour

drug-light interval (optimized for survival) (18), PDT was performed by superficial irradiation of the tumor with a 630 nm laser (Biolitec AG., A-1030, Vienna) coupled to a microlens fiber to produce a collimated beam of 1-cm diameter on the tumor surface. A total in-air fluence of 50, 135, 200, or 250 J/cm^2 was delivered at in-air fluence rates (ϕ_{air}) of 50, 75, or 150 mW/cm^2. The "in-air fluence rate" is defined as the calculated irradiance determined by laser power divided by the treatment area. The "in-air fluence" was calculated by multiplying the "in-air fluence rate" by the treatment time. Mice were randomly assigned to various treatment groups. Immediately before and after PDT, the Photofrin fluorescence in the tumor was measured using a custom-designed multi-fiber probe (19). The multi-fiber probe was in physical contact with the tumor surface. The contact probe is composed of an array of optical fibers, one of which was connected to the 405 nm excitation light to measure fluorescence at detection fibers spaced at fixed locations from the source fiber. Collected spectra were imaged by a multi-channel CCD system and analyzed by a singular value decomposition (SVD) method (20). The contact probe collects fluorescence light only up to the depth of penetration of the UV excitation laser and the area of contact. The absorption coefficient (μ_a) and reduced scattering coefficient (μ_s') of the tumor tissue was also obtained pre- and post-PDT using a two-catheter method (21). Tumor-bearing mice that received neither light irradiation nor Photofrin were used as controls. All procedures were approved by the Institutional Animal Care and Use Committee of University of Pennsylvania. Animal husbandry was provided by the Laboratory Animal Resources of the University of Pennsylvania in association with Assessment and Accreditation of Laboratory Animal Care (AALAC).

Determination of Photofrin concentration from the fluorescence measurements

Photofrin fluorescence spectra were measured using a multi-fiber spectroscopic contact probe (19) and were analyzed using singular value decomposition (SVD) fitting (20). The conversion between the best –fit value of the Photofrin component and *in vivo* Photofrin concentration was obtained by comparing the *in vivo* fluorescence with that of phantoms with known photosensitizer concentrations. An empirical correction factor was obtained from the phantom experiments and varying μ_a and μ_s' (22). In separate experiments, the accuracy of the *in vivo* measurements were evaluated. Mice with tumors were administered Photofrin at a 24 hour drug-light interval and the interstitial photosensitizer concentration was measured with the multi-fiber probe. Immediately afterwards, tumors were excised and frozen. Tumors were later homogenized with Soluble (Perkin Elmer, Waltham, Massachusetts, United States) and their fluorescence was measured by a spectrofluorometer (FluoroMax-3; Jobin Yvon, Inc., Edison, New Jersey, United States). An excitation of 405 nm was used with an emission range from 630–750 nm, and photosensitizer concentration in tissue was calculated based on the increase in fluorescence resulting from the addition of a known amount of Photofrin to each sample after its initial reading. The correlation between the *in vivo* and *ex vivo* measurements was found to follow a linear fit ($y=x$) with goodness of $R^2 = 0.99$ (22).

Calculation of the tumor local control rate (LCR)

The width (a) and length (b) of the tumors were measured daily using a sliding caliper for up to 14 days post-PDT. The tumor volumes (V) were calculated using $V = \pi \times a^2 \times b/6$ (23). The

raw tumor volumes were fitted to V_0e^{kd} for individual mouse (23). Since initial tumor volumes (V_0) at the time of treatment were not identical among mice (12 to 50 mm^3), daily tracked tumor volumes were scaled relative to an initial normalized tumor volume of ~ 23 mm^3 (the average of all initial tumor volume). This process provided for consistent comparisons among treatment groups. PDT was performed at small tumor volume to ensure complete treatment of the entire tumor (light can penetrate 3 – 5 mm depth), providing the potential for a curative response. To treat larger tumor volumes to complete cures would require interstitial delivery of light. This process provided for consistent comparisons among treatment groups. Tumors were randomly assigned to various treatment groups. A Kaplan–Meier curve for *LCR* was generated based on a tumor volume ≤ 50 mm^3 and stratefied based on three different dosimetric metrics (fluence, PDT dose, and $[^1O_2]_{rx}$). A tumor volume of 50 mm^3 was chosen as the endpoint because this volume enabled clear discrimination of tumor recurrence from treatment-induced inflammation in the two week period after PDT over which this study was conducted.

Calculation of the reacted singlet oxygen and PDT dose during PDT

The longitudinal distribution of ϕ for the 1-cm diameter field was determined using a Monte-Carlo (MC) simulation for a known in-air fluence rate and individual mouse tissue optical properties (22). The mean mouse tissue optical properties for the group was: μ_a = 0.9 cm^{-1} and μ'_s = 8.4 cm^{-1}, which if used to replace the actual tissue optical properties will introduce ~10 % error in ϕ at 3 mm depth among different mice in the population (22). To obtain the corresponding temporal changes of Photofrin concentration ($[S_0]$), oxygen concentration ($[^3O_2]$), and $[^1O_2]_{rx}$, the ϕ distribution and the measured photosensitizer concentration were passed to the following time (t)-dependent differential equations for a given treatment time point:

$$\frac{d[S_0]}{dt}+\left(\xi\sigma\frac{\phi([S_0]+\delta)[^3O_2]}{[^3O_2]+\beta}\right)[S_0]=0, \quad (1)$$

$$\frac{d[^3O_2]}{dt}+\left(\xi\frac{\phi[S_0]}{[^3O_2]+\beta}\right)[^3O_2]-g\left(1-\frac{[^3O_2]}{[^3O_2](t=0)}\right)=0, \quad (2)$$

$$\frac{d[^1O_2]_{rx}}{dt}-\left(\xi\frac{\phi[S_0][^3O_2]}{[^3O_2]+\beta}\right)=0. \quad (3)$$

The definition and value of the specific PDT photochemical parameters (ξ, σ, β, δ, and g) are listed in Table 1. Initial oxygenation concentration ($[^3O_2]_0$) is assumed to be 40 μM (13, 24). All calculations were performed using MATLAB R2015b (Mathworks®, Natick, Massachusetts, United States). More details of the calculation can be found elsewhere (17,

22). $[^1O_2]_{rx}$ is determined using Eq. 3 at a depth of z = 3 mm. The PDT dose at z = 3 mm is calculated as:

$$D(Z)=\int_0^T \phi(z,t)[S_0](t)dt \quad (4)$$

For simplicity, we use the term “fluence” to refer to “in-air fluence” as a dosimetry quantity, and “PDT dose” and $[^1O_2]_{rx}$ refer to PDT dose and $[^1O_2]_{rx}$ calculated at z = 3 mm tumor depth, respectively, in the text.

Statistical Analysis

The association of light fluence, PDT dose, and $[^1O_2]_{rx}$ with treatment efficacy was evaluated by Kaplan-Meier and statistical analyses; *LCR* was considered as the treatment endpoint. The Kaplan-Meier curves for *LCR* based on each PDT dose metrics group (fluence, PDT dose, and $[^1O_2]_{rx}$) were compared with the use of log-rank test. To explore how well the three dose metrics predict *LCR* at 7 and 14 days, the logistic regression procedure (25) was used with the dose metrics as continuous predictors. The goodness-of-fit (predictive power) for the logistic regression models were quantified by the max-rescaled generalized R^2 statistic (25, 26), which can be interpreted as the proportion of variations in *LCR* that is predicted by each dose metric. The overall predictive power of the three dose metrics was analyzed by the Cox proportional hazard model (27) with dose metrics treated as continuous predictors. The Cox model characterizes how well the dose metrics predict *LCR* over time from day 1 to day 14. The overall predictive power of the three dose metrics was also assessed by the max-rescaled generalized R^2 statistic of the corresponding Cox models. The marginal predictive powers of the three dose metrics were investigated by using each metric as the only predictor. We then estimated the multivariate associations by involving more than one dose metric into the Cox model. We tested the significance of one dose metric by controlling one or two other dose metrics, with the use of the Wald chi-square test. We also tested whether the survival probability could be better predicted by adding one or more dose metrics, based on the likelihood ratio tests. The analysis was conducted with the use of SAS software (version 9.4), and all p-values were two-sided. For the analyses $p<0.05$ level (95% confidence level) was considered statistically significant.

RESULTS

With the same Photofrin injected dose of 5 mg/kg, the uptake of Photofrin in tumors varied widely from 0.95 to 10.53 μM (3.54 μM median value). Mice that received a dose of 15 mg/kg Photofrin had tumors levels of Photofrin that ranged from 2.12 to 12.62 μM (7.08 μM median value). Variation of this magnitude is seen in the intraperitoneal tumors of human patients as well (28). Animals were assigned to four light fluence groups, and each group was comprised of 2–3 subgroups with different ϕ. Tables 2, 3, and 4 summarize the results when the mice were stratified by fluence, PDT dose, and $[^1O_2]_{rx}$, respectively.

The raw tumor regrowth data for each PDT treatment and control group was fitted to an exponential function ($V_0 e^{-kd}$) and then normalized to the mean intial mean volume, 23 mm^3. The normalized regrowth data by multiplying all data by $23/V_0$ are shown in Fig. 1.

The association of light fluence, PDT dose, and $[^1O_2]_{rx}$, with treatment efficacy was evaluated by Kaplan-Meier analyses; *LCR* was considered as the treatment endpoint. As shown in Fig. 2(a), fluence was the poorest among these three metrics. Tumor control improved with a light fluence of 135, 250, 200 and 50 J/cm^2, in that order. Thus, light fluence did not well correlate with outcome. Figures 1(b) and 1(c) show the relationship of PDT dose and $[^1O_2]_{rx}$ with tumor response; the mice were grouped into four ranges of calculated PDT dose and $[^1O_2]_{rx}$. As shown in these figures, *LCR* increased with an increase in PDT dose and $[^1O_2]_{rx}$. The log-rank tests showed significant differences among the stratified Kaplan-Meier curves for all dose metrics in Fig. 2, see statistics analysis summarized in Table 5.

The *LCR* at 7 and 14 days were further plotted by grouping the three dose metrics into 5 or 6 groups in Fig. 3 to show the predictive power of each dosimetric quantity. The solid lines were fits to the data using a sigmoid curve (y = 100 / (1 + exp (*b* - *c x*))).

DISCUSSION

The variation of the initial tumor volumes (12–55 mm^3) between different tumors within the same treatment condition could introduce variations on local tumor control. This can be caused by tumor growth rate difference or can be caused by the variation of the starting date for PDT treatment for each mouse. To minimize these effects, we have fitted the tumor growth for each PDT treatment group of mice to an exponential fucntion ($V_0 e^{-kd}$) and then normalized the initial tumor volume to the mean initial tumor volume (23 mm^3) as shown in Fig. 1.

Based on a series of light fluences and ϕ, the effectiveness of Photofrin-mediated PDT on tumor *LCR* was investigated. Kaplan–Meier curves for *LCR* were chosen to assess Photofrin-mediated PDT treatment outcome because each dosimetrical condition exhibits a probability of treatment outcome, unlike what was found for some other photosensitizers where a more definitive outcome is observed (29). The Kaplan-Meier curves for Photofrin-mediated PDT found large variations in treatment response when mice were separated based on light fluence (Figs. 2a and 3a), which is a clear indication that light fluence alone is not predictive of PDT outcome. This conclusion is in agreement with that reported by others (8). However, some correlation between fluence and tumor response would likely emerge if the fluence range were increased. As indicated previously, PDT dose was better correlated to *LCR* than fluence (8). The correlation of $[^1O_2]_{rx}$ with *LCR* indicated that when $[^1O_2]_{rx} \geq 1.1$ mM, tumors exhibited a complete response (defined as a normalized tumor volume of ≤ 50 mm^3 at 14 days after PDT). Two different administered doses of Photofrin were used in order to produce a range in the calculated PDT dose. In Figs. 1 (a) and 2(a), the *LCR* was better after treatment at fluence 135 J/cm^2 and fluence rate 75 mW/cm^2 compared to 200 J/cm^2, 50 and 150 mW/cm^2. This can be explained by greater photosensitizing drug uptake in the mice that went on to be treated at 135 J/cm^2 and 75 mW/cm^2, compared to those who

were treated at 200 J/cm^2, 50 and 150 mW/cm^2, specifically the photosensitizer uptake happened to be 3 and 2 times higher than the other sets of experiments (see Tables 2–4). It is also in general 3 times higher than the average uptake of the entire mice.

The Cox proportional hazard models were fitted to quantify the overall predictive power of the three dose metrics by treating the dose metrics as continuous predictors of *LCR* over the whole time interval from day 1 to day 14. The results are shown in Table 5. Light fluence explained 24% of the variations in *LCR* over the whole time interval (R^2 = 0.2414). PDT dose explained 43% of the variations in *LCR* over the whole time interval (R^2 = 0.4295). $[^1O_2]_{rx}$ explained 49% of the variations in *LCR* over the whole time interval (R^2 = 0.4919). These results indicate that, as a predictor of treatment outcome, $[^1O_2]_{rx}$ is better correlated with tumor response than PDT dose, and PDT dose is better correlated with tumor response than is the fluence. The $[^1O_2]_{rx}$ and the PDT dose are associated with less subject-to-subject variation in response. In multivariate models, the model combining fluence and PDT dose significantly outperforms the marginal models of the two dose metrics ($p < 0.0001$ for fluence and $p = 0.0183$ for PDT dose). Fluence is still a significant predictor ($p = 0.0019$) after controlling PDT dose. The model combining fluence and $[^1O_2]_{rx}$ significantly outperforms the marginal model of fluence ($p < 0.0001$); but it is not significantly better than the marginal model of $[^1O_2]_{rx}$ ($p = 0.9822$). Fluence is no longer a significant predictor ($p = 0.9824$) after controlling $[^1O_2]_{rx}$. The R^2 value of the model containing both fluence and $[^1O_2]_{rx}$ is virtually the same as the marginal model of $[^1O_2]_{rx}$, which means light fluence adds no value to the prediction of survival probability if $[^1O_2]_{rx}$ is given. The model combining PDT dose and $[^1O_2]_{rx}$ significantly outperforms the marginal models of the two dose metrics ($p = 0.0004$ for PDT dose and $p = 0.0477$ for $[^1O_2]_{rx}$. But PDT dose is no longer a significant predictor ($p = 0.0805$) after controlling $[^1O_2]_{rx}$. The full model that contains all three dose metrics is significantly better than all the models without $[^1O_2]_{rx}$; but it is not significantly better than the marginal model of $[^1O_2]_{rx}$ ($p = 0.1360$) or the bivariate model containing both PDT dose and $[^1O_2]_{rx}$ ($p = 0.7913$). In the full model, fluence ($p = 0.7936$) and PDT dose ($p = 0.0798$) are not significant predictors after controlling $[^1O_2]_{rx}$ ($p = 0.0056$).

The threshold value of PDT dose for achieving complete tumor control was 1200 μM J/cm^2 for Photofrin. This value is equivalent to 4.2 J/cm^3 absorbed dose, calculated by multiplying the threshold value by the extinction coefficient of Photofrin. An absorbed dose of 4.2 J/cm^3 for Photofrin is reasonably in agreement with 5.7, and 4.1 J/cm^3 absorbed dose by 2-(1-Hexyloxyethyl)-2-devinylpyropheophorbide (HPPH) (30) and benzoporphyrin derivative monoacid ring A (BPD) (31), respectively (see Table 6). These values correspond to 13.4×10^{18}, 19×10^{18}, and 14.3×10^{18} photons/cm^3 (calculated by dividing by the energy per photon) for Photofrin, HPPH and BPD, respectively. The PDT dose threshold behavior for our current results is larger than the 3.4×10^{18} photons/cm^3 reported by others for Photofrin *in vitro* (32, 33). Although PDT dose accounts for both light fluence and tissue Photofrin level, it does not account for the oxygen dependence of singlet oxygen quantum yield and thus overestimates the production of $[^1O_2]_{rx}$ in hypoxic conditions.

We also demonstrated that the threshold dose of $[^1O_2]_{rx}$ to achieve complete tumor control was 1.1 mM for Photofrin. This value is comparable to the threshold of 1.2 mM and 1.15

mM to achieve tumor control for HPPH-PDT(30) and BPD-PDT (31), respectively (see Table 4). Our previous studies demonstrated that the threshold dose of $[^1O_2]_{rx}$ to produce necrosis in the RIF tumor model was about 0.74 ± 0.25 mM for Photofrin-mediated PDT, 0.6 ± 0.1 for HPPH-mediated PDT (17, 13), 0.67 ± 0.13 for BPD-mediated PDT (29). However, it is likely that the mean values of $[^1O_2]_{rx}$ for producing tumor cure is larger than that needed to induce tumor necrosis. These results show that mean $[^1O_2]_{rx}$ at a 3 mm tumor depth is a good dosimetric quantity that combines the explicit dosimetry of light fluence and photosensitizer concentration, along with model calculation (Eqs. 1–3) of oxygen consumption during PDT.

The *LCR* at 7 and 14 days were further correlated with the three dose metrics in Fig. 3 to show the predictive power of each dosimetric quantity. Logistic regression models were fitted to *LCR* at 7 and 14 days with the three dose metrics as continuous predictors. Light fluence explained 23% of the variations in *LCR* at 7 days (R^2 = 0.2260) and 20% of the variations in *LCR* at 14 days (R^2 = 0.1976). PDT dose explained 62% of the variations in *LCR* at 7 days (R^2 = 0.6156) and 52% of the variations in *LCR* at 14 days (R^2 = 0.5210). $[^1O_2]_{rx}$ explained 67% of the variations in *LCR* at 7 days (R^2 = 0.6666) and 73% of the variations in *LCR* at 14 days (R^2 = 0.7259). Based on the statistics analyses, the light fluence is not predictive of *LCR* (see Fig. 3a), while PDT dose (see Fig. 3b) and $[^1O_2]_{rx}$ (see Fig. 3c) are correlated with *LCR* at both 7 days and 14 days; the two track each other very well. In comparisons of PDT dose and $[^1O_2]_{rx}$ as dose metrics, $[^1O_2]_{rx}$ predicts complete response at 14 days (R^2 = 0.7259) better than PDT dose (R^2 = 0.5210). When $[^1O_2]_{rx}$ also is used as a dose metric, smaller light fluences are required to produce a tumor response than when PDT dose is used (for equivalent photosensitizer uptake) (see Tables 3 and 4).

One limitation of the current study is that the $[^1O_2]_{rx}$ is calculated using Eqs. 1–3 rather than based on the actual measured tissue oxygen concentration during PDT. We anticipate improved prediction of *LCR* if the $^3O_2$ concentration variation during PDT can be incorporated directly into the $[^1O_2]_{rx}$ determination.

CONCLUSIONS

The predictive ability of fluence, PDT dose, and $[^1O_2]_{rx}$ as dosimetric quantities was evaluated by analyzing their relationships with *LCR*. Based on the outcomes of this study, $[^1O_2]_{rx}$ is better than PDT dose, which in turn is better than light fluence, in predicting tumor control for Photofrin-mediated PDT. In addition, PDT dose requires a higher fluence than that predicted by $[^1O_2]_{rx}$ for the same photosensitizer uptake to achieve a complete tumor response.

Acknowledgments

This work is supported by grants from the National Institute of Health (NIH), R01 CA154562 and P01 CA87971.

References

1. Dougherty TJ, Gomer CJ, Henderson BW, Jori G, Kessel D, Korbelik M, Moan J, Peng Q. Photodynamic therapy. J Natl Cancer Inst. 1998; 90:889–905. [PubMed: 9637138]

2. Gross SA, Wolfsen HC. The role of photodynamic therapy in the esophagus. Gastrointest Endosc Clin N Am. 2010; 20:35–53. vi. [PubMed: 19951793]

3. Corti L, Toniolo L, Boso C, Colaut F, Fiore D, Muzzio PC, Koukourakis MI, Mazzarotto R, Pignataro M, Loreggian L, Sotti G. Long-term survival of patients treated with photodynamic therapy for carcinoma in situ and early non-small-cell lung carcinoma. Lasers Surg Med. 2007; 39:394–402. [PubMed: 17565719]

4. Simone CB 2nd, Cengel KA. Photodynamic therapy for lung cancer and malignant pleural mesothelioma. Semin Oncol. 2014; 41:820–830. [PubMed: 25499640]

5. Hu XH, Feng Y, Lu JQ, Allison RR, Cuenca RE, Downie GH, Sibata CH. Modeling of a type II photofrin-mediated photodynamic therapy process in a heterogeneous tissue phantom. Photochem Photobiol. 2005; 81:1460–1468. [PubMed: 15960591]

6. Castano AP, Demidova TN, Hamblin MR. Mechanisms in photodynamic therapy: part one-photosensitizers, photochemistry and cellular localization. Photodiag Photodyn Ther. 2004; 1:279–293.

7. Dolmans DE, Fukumura D, Jain RK. Photodynamic therapy for cancer. Nat Rev Cancer. 2003; 3:380–387. [PubMed: 12724736]

8. Wang HW, Rickter E, Yuan M, Wileyto EP, Glatstein E, Yodh A, Busch TM. Effect of photosensitizer dose on fluence rate responses to photodynamic therapy. Photochem Photobiol. 2007; 83:1040–1048. [PubMed: 17880498]

9. Sitnik TM, Hampton JA, Henderson BW. Reduction of tumour oxygenation during and after photodynamic therapy in vivo: effects of fluence rate. Br J Cancer. 1998; 77:1386–1394. [PubMed: 9652753]

10. Hopper C. Photodynamic therapy: a clinical reality in the treatment of cancer. Lancet Oncol. 2000; 1:212–219. [PubMed: 11905638]

11. Zhou X, Pogue BW, Chen B, Demidenko E, Joshi R, Hoopes J, Hasan T. Pretreatment photosensitizer dosimetry reduces variation in tumor response. IJROBP. 2006; 64:1211–1220.

12. Rizvi I, Anbil S, Alagic N, Celli J, Zheng LZ, Palanisami A, Glidden MD, Pogue BW, Hasan T. PDT dose parameters impact tumoricidal durability and cell death pathways in a 3D ovarian cancer model. Photochem Photobiol. 2013; 89:942–952. [PubMed: 23442192]

13. Penjweini R, Liu B, Kim MM, Zhu TC. Explicit dosimetry for 2-(1-hexyloxyethyl)-2-devinyl pyropheophorbide-a-mediated photodynamic therapy: macroscopic singlet oxygen modeling. J Biomed Opt. 2015; 20:128003. [PubMed: 26720883]

14. Niedre M, Patterson MS, Wilson BC. Direct near-infrared luminescence detection of singlet oxygen generated by photodynamic therapy in cells in vitro and tissues in vivo. Photochem Photobiol. 2002; 75:382–391. [PubMed: 12003128]

15. Wang KK, Mitra S, Foster TH. A comprehensive mathematical model of microscopic dose deposition in photodynamic therapy. Med Phys. 2007; 34:282–293. [PubMed: 17278514]

16. Jarvi MT, Patterson MS, Wilson BC. Insights into photodynamic therapy dosimetry: simultaneous singlet oxygen luminescence and photosensitizer photobleaching measurements. Biophys J. 2012; 102:661–671. [PubMed: 22325290]

17. Wang KK, Finlay JC, Busch TM, Hahn SM, Zhu TC. Explicit dosimetry for photodynamic therapy: macroscopic singlet oxygen modeling. J Biophotonics. 2010; 3:304–318. [PubMed: 20222102]

18. Li LB, Luo RC. Effect of drug–light interval on the mode of action of Photofrin photodynamic therapy in a mouse tumor model. Lasers Med Sci. 2009; 24:597–603. [PubMed: 18936869]

19. Gallagher-Colombo SM, Quon H, Malloy KM, Ahn PH, Cengel KA, Simone CB, Chalian AA, O'Malley BW, Weinstein GS, Zhu TC, Putt ME, Finlay JC, Busch TM. Measuring the Physiologic Properties of Oral Lesions Receiving Fractionated Photodynamic Therapy. Photochem Photobiol. 2015; 91:1210–1218. [PubMed: 26037487]

20. Finlay JC, Conover DL, Hull EL, Foster TH. Porphyrin bleaching and PDT-induced spectral changes are irradiance dependent in ALA-sensitized normal rat skin in vivo. Photochem Photobiol. 2001; 73:54–63. [PubMed: 11202366]

21. Dimofte A, Finlay JC, Zhu TC. A method for determination of the absorption and scattering properties interstitially in turbid media. Phys Med Biol. 2005; 50:2291–2311. [PubMed: 15876668]
22. Qiu H, Kim MM, Penjweini R, Zhu TC. Macroscopic singlet oxygen modeling for dosimetry of Photofrin-mediated photodynamic therapy- an in-vivo study. J Biomed Opt. 2016; 21:088002.
23. Busch TM, Xing X, Yu G, Yodh A, Wileyto EP, Wang HW, Durduran T, Zhu TC, Wang KK. Fluence rate-dependent intratumor heterogeneity in physiologic and cytotoxic responses to Photofrin photodynamic therapy. Photochem Photobiol Sci. 2009; 8:1683–1693. [PubMed: 20024165]
24. Whiteley JP, Gavaghan DJ, Hahn CE. Mathematical modelling of oxygen transport to tissue. J Math Biol. 2002; 44:503–522. [PubMed: 12111100]
25. Cox, DR., Snell, EJ. The analysis of binary data. Chapman and Hall/CRC; New York, NY: 1989.
26. Nagelkerke NJD. A note on a general definition of the coefficient of determination. Biometrika. 1991; 78:691–692.
27. Cox DR. Regression models and life-tables (with discussion). J R Stat Soc Ser B. 1972; 34:187–220.
28. Wang HW, Zhu TC, Putt ME, Solonenko M, Metz J, Dimofte A, Miles J, Fraker DL, Glatstein E, Hahn SM, Yodh AG. Broadband reflectance measurements of light penetration, blood oxygenation, hemoglobin concentration, and drug concentration in human intraperitoneal tissues before and after photodynamic therapy. J Biomed Opt. 2005; 10:014004.
29. Kim MM, Penjweini R, Liang X, Zhu TC. Explicit macroscopic singlet oxygen modeling for benzoporphyrin derivative monoacid ring A (BPD)-mediated photodynamic therapy. J Photochem Photobiol B: biol. 2016; 164:314–322.
30. Penjweini R, Kim MM, Liu B, Zhu TC. Evaluation of the 2-(1-Hexyloxyethyl)-2-devinyl pyropheophorbide (HPPH) mediated photodynamic therapy by macroscopic singlet oxygen modeling. J Biophotonics. Sep; 2016 9(11-12):1344–1354. DOI 10.1002/jbio.201600121. [PubMed: 27653233]
31. Kim MM, Ghogare AA, Greer A, Zhu TC. On the in-vivo photochemical rate parameters for PDT reactive oxygen species modeling. Phys Med Biol. 2017; 62:R1–R48. [PubMed: 28166056]
32. Patterson MS, Wilson BC, Graff R. In vivo tests of the concept of photodynamic threshold dose in normal rat liver photosensitized by aluminum chlorosulphonated phthalocyanine. Photochem Photobiol. 1990; 51:343–349. [PubMed: 2356229]
33. Kadish KM, Smith KM, Guilard R. The Porphyrin Handbook: Applications of phthalocyanines. Academic Press, An Imprint of Elsevier, San Diego, CA. 2003; 19:16–18.
34. Georgakoudi I, Nichols MG, Foster TH. The mechanism of Photofrin photobleaching and its consequences for photodynamic dosimetry. Photochem Photobiol. 1997; 65:135–144. [PubMed: 9066293]
35. Nichols MG, Foster TH. Oxygen diffusion and reaction kinetics in the photodynamic therapy of multicell tumour spheroids. Phys Med Biol. 1994; 39:2161–2181. [PubMed: 15551546]
36. Dysart JS, Singh G, Patterson MS. Calculation of singlet oxygen dose from photosensitizer fluorescence and photobleaching during mTHPC photodynamic therapy of MLL cells. Photochem Photobiol. 2005; 81:196–205. [PubMed: 15469385]
37. Zhu TC, Liu B, Penjweini R. Study of tissue oxygen supply rate in a macroscopic photodynamic therapy singlet oxygen model. J Biomed Opt. 2015; 20:38001.
38. Carreau A, El Hafny-Rahbi B, Matejuk A, Grillon C, Kieda C. Why is the partial oxygen pressure of human tissues a crucial parameter? Small molecules and hypoxia. J Cell Mol Med. 2011; 15:1239–1253. [PubMed: 21251211]

This preclinical study examines light fluence, PDT dose, and “apparent reacted singlet oxygen”, $[^1O_2]_{rx}$, to predict local control rate (*LCR*) for Photofrin-mediated photodynamic therapy (PDT) of radiation-induced fibrosarcoma (RIF) tumors. *LCR* was stratified for different dose metrics for 74 mice (66+8 control). Complete tumor control at 14 days was observed for $[^1O_2]_{rx} \geq 1.1$mM or PDT dose ≥ 1200μMJ/cm^2 but cannot be predicted with fluence alone. *LCR* increases with increasing $[^1O_2]_{rx}$ and PDT dose but is not well correlated with fluence. Comparing dosimetric quantities, $[^1O_2]_{rx}$ outperformed both PDT dose and fluence in predicting tumor response and correlating with *LCR*.

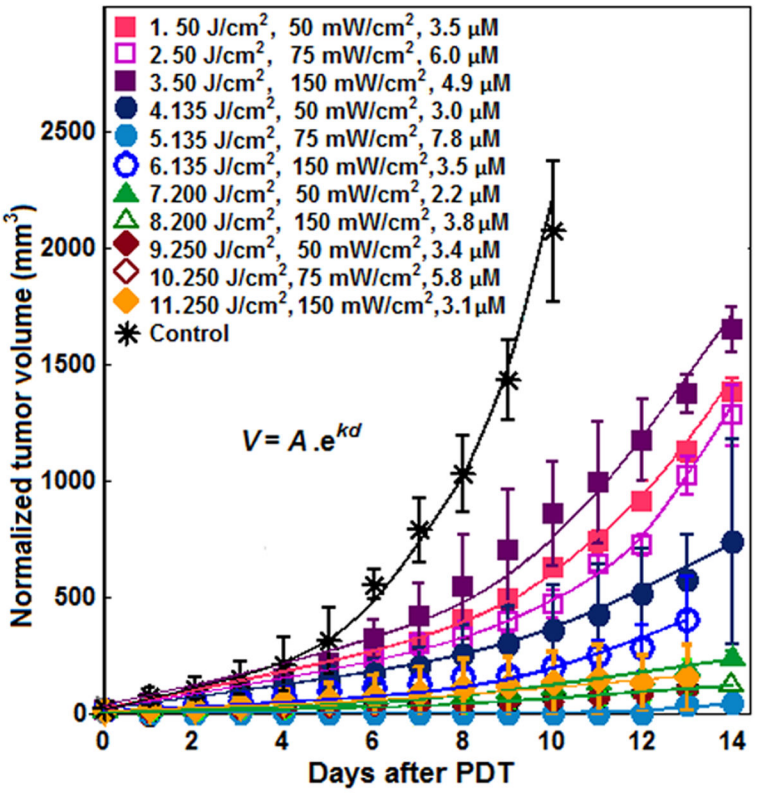

Figure 1.

Exponential fitting of the normalized tumor volume over time after PDT. The index in the legend corresponds to that in Table 2. This figure has been modified from Ref. (22) with additional data.

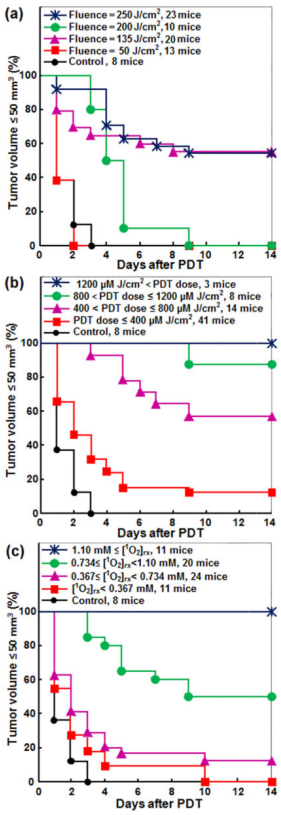

Figure 2.

The impact of a) fluence, b) PDT dose at 3 mm tumor depth, and c) reacted singlet oxygen ($[^1O_2]_{rx}$) at 3 mm tumor depth on Kaplan-Meier curves of tumor local control rate (*LCR*) after Photofrin-mediated PDT. A normalized tumor volume ≤ 50 mm^3 was used as the endpoint. The solid dark blue line with star symbols in (b) and (c) corresponds to the complete control of tumors.

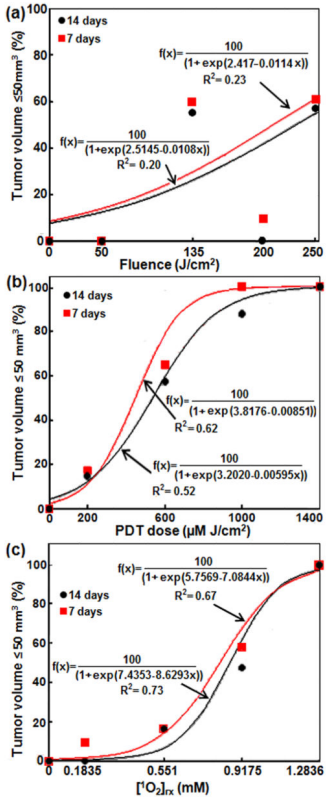

Figure 3.

Tumor local control rate (*LCR*) at 7 and 14 days *versus* (a) light fluence, (b) PDT dose at 3 mm tumor depth, (c) $[^1O_2]_{rx}$ at 3 mm tumor depth. The solid lines are the sigmoid function (y=100/(1+ exp(b-cx)) for (b) and (c) fits, the resulting goodness of fits are R^2 = 0.20 (0.33), 0.52 (0.68), 0.72 (0.72) for light fluence, PDT dose at 3 mm, and $[^1O_2]_{rx}$ at 3 mm for *LCR* at 14 (7) days, respectively.

Table 1

Photofrin photochemical parameters used in the macroscopic kinetic equations.

Parameter	Definition	Value	References
ξ ($cm^2s^{-1}mW^{-1}$)	Specific oxygen consumption rate	3.7×10^{-3}	(34, 35, 17)
σ (μM^{-1})	Specific photobleaching ratio	7.6×10^{-5}	(17, 34)
β (μM)	Oxygen quenching threshold concentration	11.9	(34)
δ (μM)	Low concentration correction	33	(36)
g (μM/s)	Macroscopic oxygen maximum perfusion rate	0.76	(17)
$[^3O_2]_0$ (μM)	Initial ground-state oxygen concentration	40	(37, 13, 24, 38)

Table 2

In-air light fluence and in-air light fluence rate conditions used in each PDT treatment group.

Index	Fluence (J/cm^2)	ϕ_{air} (mW/cm^2)	PDT dose (μM J/cm^2)	Photofrin (μM)	Photofrin variation† (μM)	$[^1O_2]_{rx}$ (mM)	$[^1O_2]_{rx}$ variation† (mM)	Variation count†
1	**50**	50	126.5	3.5	-	0.35	-	0 / 4
2		75	235.5	6.0	-	0.40	-	0 / 5
3		150	199.9	4.9	-	0.24	-	0 / 4
4	**135**	50	229.7	3.0	2.52 / 4.33*	0.66	0.45/0.91$^{\#}$	1 / 4
5		75	774.2	7.8	3.08 / 12.1*	0.93	0.27/1.25$^{\#}$	10 / 12
6		150	322.3	3.5	-	0.53	-	0 / 4
7	**200**	50	204.8	2.2	-	0.63	-	0 / 5
8		150	417.8	3.8	-	0.76	-	0 / 5
9	**250**	50	362.1	3.4	3.17 / 3.66*	1.03	0.97 / 1.09$^{\#}$	3 / 4
10		75	1380.1	5.8	1.88 / 12.6*	0.74	0.65 / 1.32$^{\#}$	8 / 10
11		150	393.0	3.1	2.45 / 5.32*	0.81	0.69 / 1.04$^{\#}$	2 / 9
	Control	0	0	0	-	0	-	0 / 8

*Photofrin concentration in tumors with complete and partial response is significantly different, $p<0.05$.

$^{\#}[^1O_2]_{rx}$ concentration tumors with complete and partial response is significantly different, $p<0.05$

†Variation is shown for (tumors with complete response) / (total number of tumors) at 14 days.

Table 3

The amounts of PDT dose calculated for each PDT treatment condition.

PDT dose	$[^1O_2]_{rx}$ (mM)	In-air Fluence (J/cm^2)	ϕ_{air} (mW/cm^2)	Photofrin (μM)	Mice number
1200 μM J/cm^2 < PDT dose	1.3-2-2	250	75	9.9–12.6	3
800<PDT dose≤1200 μM J/cm^2	0.3–1.3	135	75	7.2–12.1	6
	1.3–1.8	250	75	5.3–7.0	2
400<PDT dose≤800 μM J/cm^2	0.6–1.02	135	75	5.5–6.7	5
	0.8	200	150	4.7–4.9	2
	1.2–1.4	250	50	1.9–4.1	2
	0.9–1.09	250	150	3.3–6.9	5
PDT dose≤400 μM J/cm^2	0.3–0.4	50	50	2.8–4.9	4
	0.4	50	75	4.3–7.5	5
	0.2–0.3	50	150	2.9–8.8	4
	0.5–0.9	135	50	2.0–4.3	4
	0.7	135	75	3.1	1
	0.5–0.6	135	150	3.0–3.8	4
	0.3–1.0	200	50	1.0–3.7	5
	0.6–0.75	200	150	2.7–3.5	3
	0.6–1.0	250	50	3.9–4.9	2
	0.6–0.8	250	75	1.9–2.7	5
	0.3–0.6	250	150	1.0–2.0	4

Table 4

The amounts of reacted singlet oxygen concentration calculated for each PDT treatment condition.

$[^1O_2]_{rx}$	PDT dose (μM J/cm^2)	In-air Fluence (J/cm^2)	Φ_{air} (mW/cm^2)	Photofrin (μM)	Mice number
1.1 mM≤$[^1O_2]_{rx}$	977–1148	135	75	10.1–12.1	4
	418–530	250	50	1.9–4.1	2
	1555–1998	250	75	5.3–12.6	5
0.734≤$[^1O_2]_{rx}$<1.1mM	324	135	50	4.3	1
	487–1029	135	75	5.5–7.2	5
	148–278	200	50	1.6–3.0	2
	390–579	200	150	3.5–4.9	3
	354	250	50	4.9	1
	254–308	250	75	2.4–2.7	3
	410–611	250	150	3.3–6.9	5
0.367≤$[^1O_2]_{rx}$<0.734mM	166	50	50	0.4	1
	210–302	50	75	5.3–7.5	4
	155–239	135	50	2.0–3.0	3
	256–688	135	75	3.1–6.7	2
	262–358	135	150	2.9–3.8	4
	165–346	200	50	1.8–3.7	2
	276–309	200	150	2.7–2.9	2
	197	250	50	3.9	1
	199–332	250	75	1.9–2.1	2
	174–227	250	150	1.5–2.0	3
$[^1O_2]_{rx}$<0.367mM	106–122	50	50	2.8–3.2	3
	165	50	75	4.3	1
	114–366	50	150	2.9–8.8	4
	974	135	75	9.1	1
	94	200	50	1.0	1
	101	250	150	1.0	1

Table 5

Marginal and Multivariate Cox models (treating Fluence, PDT dose, and $[^1O_2]_{rx}$ as continuous variables).

	DF	Estimated Coefficients			Adjusted R-square	Likelihood Ratio Tests						
		Fluence	PDT dose	$[^1O_2]_{rx}$		Null	F	P	O	F + P	F + O	P + O
Marginal models												
1. Fluence	1	0.0084			24.14%	20.33						
p-value		*<.0001*				*<.0001*						
2. PDT dose	1		0.0041		42.95%	41.26						
p-value			*<.0001*			*<.0001*						
3. 1O2	1			2.8788	49.19%	49.76						
p-value				*<.0001*		*<.0001*						
Multivariate models												
4. F + P	2	0.0044	0.0033		47.12%	46.83	26.50	5.57				
p-value		*.0019*	*.0008*			*<.0001*	*<.0001*	*.0183*				
5. F + O	2	0.0001		2.8874	49.19%	49.76	29.43		<0.01			
p-value		*.9824*		*<.0001*		*<.0001*	*<.0001*		*0.9822*			
6. P + O	2		0.0015	2.2747	51.84%	53.68		12.42	3.92			
p-value			*.0805*	*<.0001*		*<.0001*		*.0004*	*.0477*			
7. F + P + O	3	0.0006	0.0015	2.1459	51.88%	53.75	33.42	12.49	3.99	6.92	3.99	0.07
p-value		*.7936*	*.0798*	*.0056*		*<.0001*	*<.0001*	*.0019*	*.1360*	*.0085*	*.0458*	*.7913*

DF: degree of freedom; **Null:** the null model with no factors; **F:** model 1, Fluence; **P:** model 2, PDT dose; **O:** model 3, $[^1O_2]_{rx}$; **F + P:** model 4, Fluence + PDT; **F + O:** model 5, Fluence + $[^1O_2]_{rx}$; **P + O:** model 6, PDT dose + $[^1O_2]_{rx}$; **F + P + O:** model 7, Fluence + PDT dose + $[^1O_2]_{rx}$. Likelihood ratio tests compare the multivariate models to the models with the same but fewer factors. A small *p*-value means the model with more factors is significantly better than the model with fewer factors.

Table 6

PDT dose and $[^1O_2]_{rx}$ threshold for Photofrin, 2-(1-Hexyloxyethyl)-2- devinylpyropheophorbide (HPPH) (30) and benzoporphyrin derivative monoacid ring A (BPD) (31) photosensitizers.

Photosensitizers	$\varepsilon^{\dagger}$ ($\mu M^{-1}cm^{-1}$)	$\lambda^{\ddagger}$ (nm)	PDT dose threshold (μM J cm^{-2})	Photosensitizer absorbed dose		$[^1O_2]_{rx}$ (mM)	Refs.
				(J/cm^3)	($Photons/cm^3$)		
Photofrin	0.0035	630	1200	4.2	13.4×10^{18}	1.1	This study
HPPH	0.108	665	52.62	5.7	19×10^{18}	1.2	(30)
BPD	0.078	690	52.94	4.1	14.3×10^{18}	1.15	(31)

†Extinction coefficient of the photosensitizer

‡Wavelength of the excitation light